Formation of intermetallic phases in AlSi7Fe1 alloy processed under microgravity and forced fluid flow conditions and their influence on the permeability

2016 IOP Conf. Ser.: Mater. Sci. Eng. 117 012019

(http://iopscience.iop.org/1757-899X/117/1/012019)

IOP Conf. Series: Materials Science and Engineering **117** (2016) 012019 doi:10.1088/1757-899X/117/1/012019

Formation of intermetallic phases in AlSi7Fe1 alloy processed under microgravity and forced fluid flow conditions and their influence on the permeability

S Steinbach[1,a], L Ratke[2], G Zimmermann[3] and O Budenkova[4]
[1] Institut für Materialphysik im Weltraum, Deutsches Zentrum für Luft- und Raumfahrt (DLR), 51170 Köln, Germany
[2] Institut für Werkstoff-Forschung, Deutsches Zentrum für Luft- und Raumfahrt (DLR), 51170 Köln, Germany
[3] ACCESS e.V., Intzestrasse 5, 52072 Aachen, Germany
[4] SIMAP/EPM, 1130 rue de la Piscine - BP 15, 38402 St. Martin D'Heres, France

E-mail: [a] sonja.steinbach@dlr.de

Abstract. Ternary Al-6.5wt.%Si-0.93wt.%Fe alloy samples were directionally solidified on-board of the International Space Station ISS in the ESA payload Materials Science Laboratory (MSL) equipped with Low Gradient Furnace (LGF) under both purely diffusive and stimulated convective conditions induced by a rotating magnetic field. Using different analysis techniques the shape and distribution of the intermetallic phase β-Al_5SiFe in the dendritic microstructure was investigated, to study the influence of solidification velocity and fluid flow on the size and spatial arrangement of intermetallics. Deep etching as well as 3-dimensional computer tomography measurements characterized the size and the shape of β-Al_5SiFe platelets: Diffusive growth results in a rather homogeneous distribution of intermetallic phases, whereas forced flow promotes an increase in the amount and the size of β–Al_5SiFe platelets in the centre region of the samples. The β-Al_5SiFe intermetallics can form not only simple platelets, but also be curved, branched, crossed, interacting with dendrites and porosity located. This leads to formation of large and complex groups of Fe-rich intermetallics, which reduce the melt flow between dendrites leading to lower permeability of the mushy zone and might significantly decrease feeding ability in castings.

1. Introduction

Aluminium–silicon cast alloys are widely used in industry due to their low densities, low cost, and acceptable mechanical properties. The mechanical properties of aluminium alloys are, however, adversely affected by even a small amount of iron, which leads to the formation of intermetallic phases. In Al-Si-Fe alloys the β-Al_5FeSi phase is the most harmful one (detrimental to the mechanical properties of the alloy), which solidifies as long platelets [1-4]. Insight in the three-dimensional structure of the β-Al_5FeSi phase was provided by serial sectioning [5] or x-ray computed tomography (CT) [6]. Recent investigations demonstrate that the formation of the β-Al_5FeSi phase in the interdendritic region may significantly reduce the melt flow through the mush and therefore also modify the secondary dendrite arm spacing [7].

One parameter used to characterize the fluid flow in the mushy zone is permeability, i.e. a tensor measuring the ease of fluid flow through the solid network [8]. Permeability is a critical parameter for

casting models and is related to the geometry of the liquid channels and the grain morphology [9]. For columnar dendritic structures, the permeability is anisotropic due to directional nature of the dendrite arms [10]. To investigate the anisotropy of the permeability, Poirier [9] used a multilinear regression analysis of experimental data to propose an empirical relationship based on the Blake-Kozeny equation. Puncreobutr et al. [11] continued work in this area and developed an analytical expression that takes into account the effects of intermetallic particles on permeability.

To understand the effect of convective flow on the microstructure of an alloy with intermetallic phases precipitated in the mush and to understand the effect of intermetallic phase formation on permeability, directional solidification experiments with a hypoeutectic Al-Si alloy enriched in Fe under well-defined boundary conditions in microgravity environment were performed in the frame of the ESA-MAP project MICAST (MIcrostructure Formation in CASTing of Technical Al-Alloys under Diffusive and Magnetically Controlled Convective Conditions) on-board the International Space Station (ISS). In the ESA payload MSL LGF [12] AlSi7Fe1 alloy samples were directionally solidified under both purely diffusive and stimulated convective conditions induced by a Rotating Magnetic Field (RMF). This allows for systematic studies of the impact of the solidification velocity and fluid flow on the formation of intermetallic β-Al_5FeSi phase (IMP).

2. Experimental set-up and sample analysis

In the microgravity environment provided by the ISS, four rod-like samples of diameter 7.8 mm and of length 245 mm from unmodified Al-6.5wt%Si-0.93wt%Fe alloy [13] were directionally solidified in the Bridgman-type furnace insert MSL LGF (moving furnace, fixed sample) [12] in the same temperature gradient of 2 K/mm, but with different values of the furnace movement velocity: v = 0.02 mms^{-1} (MICAST1#4), v = 0.04 mms^{-1} (MICAST1#3), v = 0.06 mms^{-1} (MICAST1#2) and v = 0.08 mms^{-1} (MICAST1#1). After a certain solidified length (50 mm on average), which may allow for a steady-state columnar growth under diffusive conditions, the rotating magnetic field (RMF) was switched on. The operating frequency of 57 Hz and the magnetic field strength of 5.7 mT are sufficient to induce forced melt flow in the melt.

Axial cross-sections of the samples were investigated to determine the distribution of the intermetallic β-Al_5FeSi phase in 2D. To allow for an unambiguous identification of the β-Al_5FeSi phases a special preparation technique with a basic final polishing step was developed. As a result the β-Al_5FeSi phases appear in an intense dark colour with respect to the primary α-Al phase and the Al-Si eutectic. Digital image analysis was used for binarization of the images. The β-Al_5FeSi phases could be identified automatically and a detailed analysis of the size and distributions of the phases was performed. Figure 1 shows as an example the β-Al_5FeSi phases for MICAST1#4 sample classified in groups of different lengths, determined with image analysis using the Feret-maximum value.

For the 3D CT analysis of the intermetallic phases samples of dimension 1x1x8mm normal to the growth direction of the sample rod (8 mm in diameter) were prepared. The scans were carried out in the x-ray tomography system Phoenix nanotom® (Phoenix |X-Ray GmbH) available at DLR. The nanofocus x-ray tube coupled with a 2304×2304 pixel detector produces a volume of 2304 × 2304 × 2304 voxels. The magnification was chosen such that an effective pixel size of 1.0 µm is obtained. A total of 800 radiographs during 360 degree of sample rotation were acquired at a tension of 100 kV and a current of 135 µA. Image corrections and ring artifact corrections were applied before the final reconstruction. After image acquisition, significant post-processing was necessary to segment the three phases: primary α-Al, intermetallics, and eutectic. From these images, tomographic 3D-volumes of 1000 x 1000 x 1000 voxels with a voxel size of 1.0 µm were generated (datos|x-reconstruction software, GE Sensing and Inspection GmbH) for each prepared sample segment. One reconstruction cube was chosen in the sample center and one was chosen at the outer part of the sample. Further image analysis was performed using AvizoFire 8.1. An example of the results is shown in figure 2: The β-Al_5FeSi phases form a complex and interconnected network.

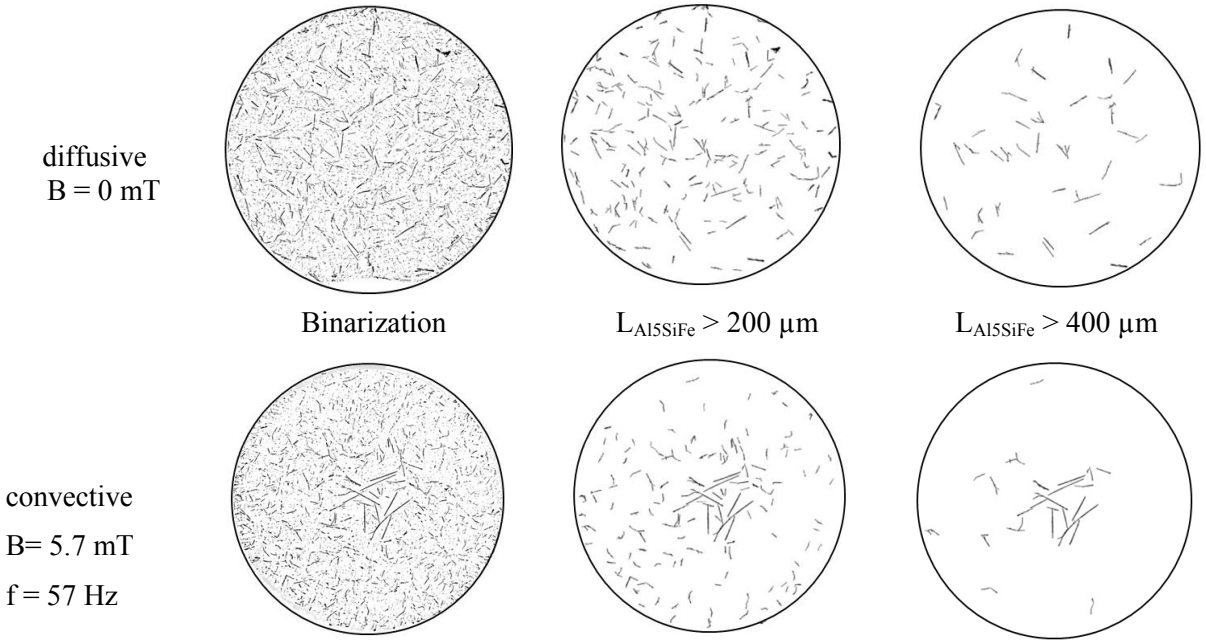

Figure 1. Binarized image (left), all β-Al_5FeSi phases longer than 200µm (middle) and all β-Al_5FeSi phases longer than 400 µm (right) of sample MICAST1#4. The top images represent diffusive growth conditions and bottom images are results of solidification with forced melt flow. The areas represent the entire rod diameter.

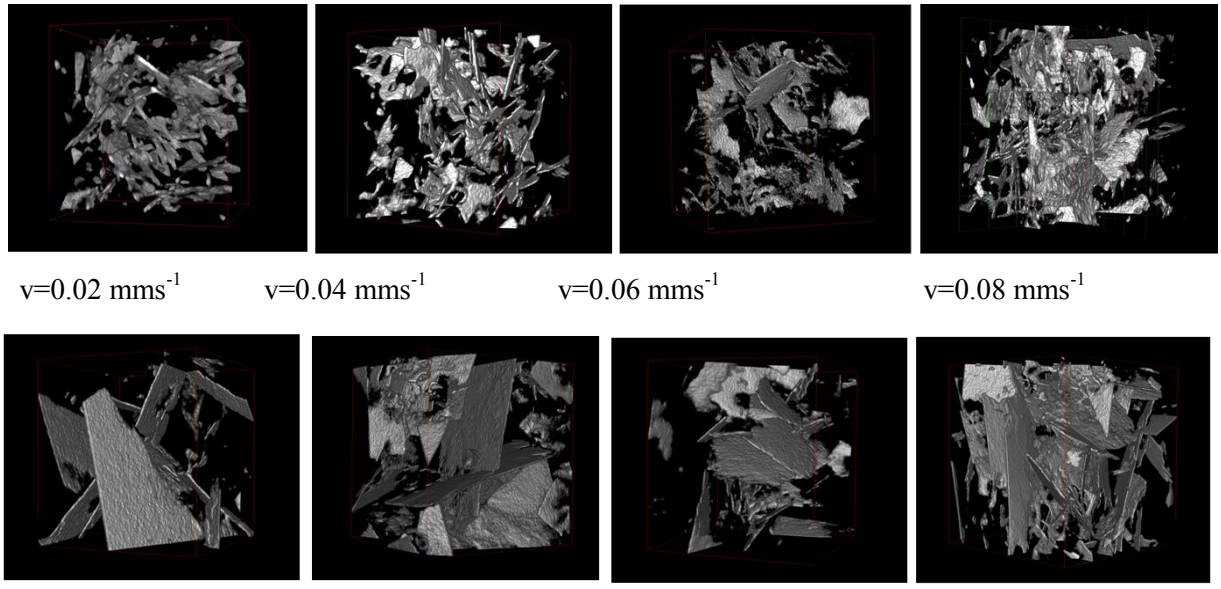

Figure 2. Segmented reconstruction cubes of 650 x 650 x 650 µm³ of samples processed with controlled melt flow and different furnace movement velocities. Top images were taken from the outer parts of the sample and bottom images were taken from the sample center.

In order to determine the influence of the intermetallic phases on the permeability of the dendritic network, the flow problem based on the Stokes equations was simulated using the reconstructed cubes (outer part of samples solidified with RMF). The commercial computational flow dynamics software Avizo XLab Hydro (VSG, France), which utilizes a finite volume method, was applied directly to the

tomographic datasets for flow predictions. The flow studies were performed in each of the three directions along the x, y and z axes of the 3D-volume. Inlet flow along the z-axis gives the permeability for liquid flow parallel to the primary dendrite arms, while permeability in the normal direction was taken as the value calculated with inlet flows along the x- and y-axes. The boundary conditions were: free pressure outlet, no-slip conditions, liquid viscosity was given a value of 0.00125Pa s.

3. Results and Discussion

3.1. 2D-analysis

Based on axial 2D cross-sections obtained from regions of pure diffusive growth and also from regions solidified with forced melt flow, the sizes and distribution of β-Al_5FeSi phases were determined for different solidification velocities (figure 1). In the diffusive case [14] the phases are larger and more homogeneously distributed than in the case of induced melt flow. In general, the size of the β-Al_5FeSi phases growing in the interdendritic region is limited by the spacing of the dendritic area and the total amount of Fe available for formation of the intermetallic phase. The RMF induced a secondary melt flow [15], which results in an enrichment of Si and Fe in the centre part of the samples due to strong macrosegregation. Therefore, especially for lower solidification velocities (figure 2, bottom left), the enrichment of Si and Fe in the sample centre part results in a few but rather large β-Al_5FeSi particles.

3.2. 3D-analysis

As seen in figure 2 the intermetallics are large and plate-like. They form a complex and interconnected network. It is immediately clear that they are able to block flow through the interdendritic network of channels (‘barrier effect’). The volume fraction of the β-Al_5FeSi phase measured for the different samples (solidified with RMF, outer part of the sample) compared to the calculated one (dashed line) is shown in figure 3. The decrease of the volume fraction at 0.02 mms^{-1} and the increase at 0.08 mms^{-1} can be explained by the local decrease and increase of the Fe content as measured by SEM EBSD microprobe analysis, respectively.

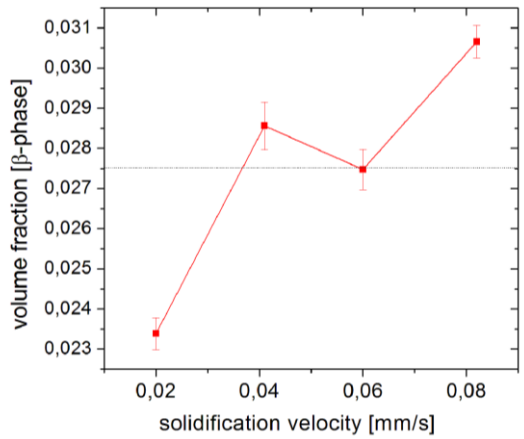

Figure 3. Volume fraction of the β-Al_5FeSi phase measured on the out of centre part of samples solidified with RMF.

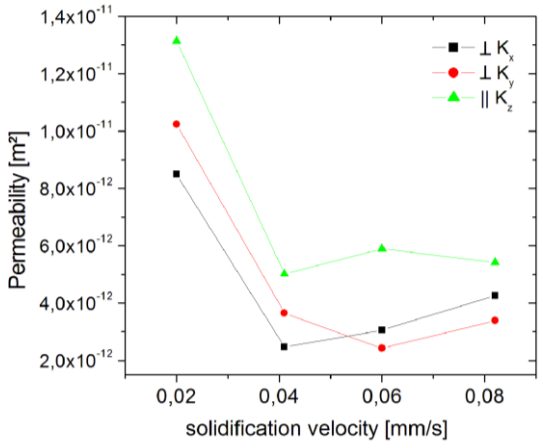

Figure 4. Permeability for liquid flow parallel (z) and perpendicular (x, y) to the primary dendrites simulated with Avizo XLab Hydro.

The permeability values extracted from the flow simulations with Avizo XLab Hydro are shown in figure 4 for flow parallel (z) and perpendicular (x, y) to the primary columnar dendrites. With decreasing solidification velocity (larger primary dendrite spacing) and decreasing volume fraction of the β-Al_5FeSi phase, the permeability increases.

The calculated permeability value (z-direction; MICAST1#2) has been fitted (figure 5) to an empirical relationship based on the Blake-Kozeny equation following the procedure of Poirier [9] and Puncreobutr [11] with an additional term, $1\text{-}\beta f_{IMP}$, where β represents the impact factor of the intermetallic phase:

$$K_p = (1 - \beta f_{IMP}) K_p^{orig} \quad (1)$$

$$K_p^{orig} = C_1 (f_l^3 \lambda_1^2)/(1 - f_l) \quad (2)$$

where K_p is the permeability in the direction parallel to the primary dendrites, K_p^{orig} is the original expression of Poirier [9], λ_1 is the primary dendrite spacing, f_l is the liquid volume fraction and C_1 is a fitting constant. The values for f_l and f_{IMP} were obtained from thermodynamic calculations with a linearized phase diagram [16]. It can be seen that in the first solidification phase the permeability decreases monotonically with temperature as expected because of the thickening of the primary dendrites as solidification progresses. The permeability is significantly lower for the case with fluid flow as compared to the one without, because of the reduced primary dendrite spacing. During the solidification phase, after the beginning of intermetallic phase precipitation, the loss of permeability that occurs due to the intermetallic phases can be directly attributed to the barrier effect of the β-Al_5FeSi phases. A further analysis is ongoing, trying to answer the question, why the effect is not bigger (grid size of the Avizo model etc.).

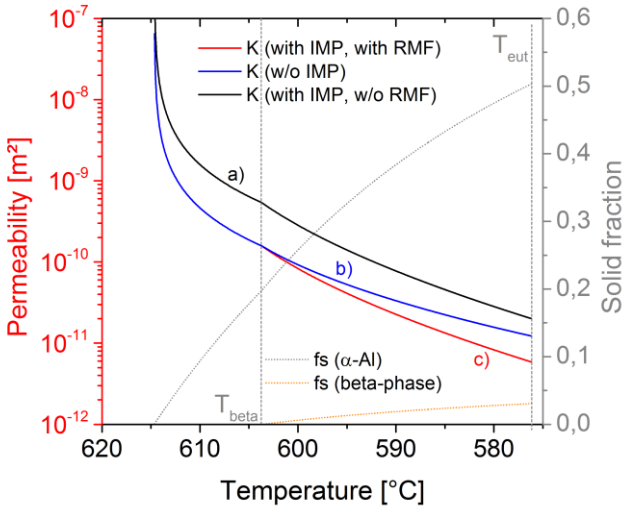

Figure 5. The evolution of permeability with temperature for flow parallel to the primary columnar dendrites a) without fluid flow but with IMP, b) with fluid flow but without IMP and c) with IMP and fluid flow (MICAST1#2). For comparison the evolution of the fraction solid of the α-Al dendrites and the β-Al_5FeSi phase with temperature is also provided. The dotted line indicates the temperature where the nucleation of the intermetallic phases started.

4. Conclusions

This paper provides an analysis of the formation of intermetallic phases in AlSi7Fe1 alloy in samples processed onboard the ISS. Based on the axial 2D cross-sections obtained from regions of purely diffusive growth and also from regions solidified under forced melt flow, the sizes and distribution of β-Al_5FeSi phases were determined for different solidification velocities. In the diffusive case the phases are larger and more homogeneously distributed than in the case of induced melt flow. Especially for lower solidification velocities, the enrichment of Si and Fe in the centre part of the sample by fluid flow results in only a few but rather large β-Al_5FeSi platelets.

The coupling of the 3D CT analysis of the structure of the β-Al_5FeSi particles, with numerical simulations demonstrates qualitatively the blocking effect of intermetallics on fluid flow and the loss in permeability in the direction parallel to the primary dendrites. This can explain the decrease in the feeding abilities in castings and could therefore explain the increased susceptibility of such alloys for casting defects as hot tearing and microporosity.

Acknowledgments
This work was conducted within the ESA-MAP programme MICAST', contract 14347/01/NL/SH, and also funded by the German Space Agency DLR. The sample material was kindly provided by Hydro Aluminium Deutschland GmbH, Bonn, Germany. The authors would like to thank the MICAST team for fruitful discussions.

References
[1] Murali S, Raman K S and Murty K S S 1994 *Materials Characterization* **33** 99
[2] Tang S K and Sritharan T 1998 *Materials Science and Technology* **14** 738
[3] Steinbach S and Ratke L 2007 *Transactions of the Indian Institute of Metals* **60** 137
[4] Mikolajczak P and Ratke L 2011 *Materials Science and Engineering* **27** 012024
[5] Dinnis C M, Taylor J A and Dahle A K 2005 *Scripta Materialia* **53** 955
[6] Terzi S, Taylor J A, Cho Y H, Salvo L, Suery M, Boller E and Dahle A K 2010 *Acta Materialia* **58** 5370
[7] Steinbach S und Ratke L 2009 *International Journal of Cast Metals Research* **22** 1
[8] Flemings M C 1974 *Solidification processing* New York, McGraw-Hill
[9] Poirier D R 1987 *Metallurgical Transactions* **18** 245
[10] Murakami K, Shiraishi A, Okamoto T 1983 *Acta Metallurgica* **31** 1417
[11] Puncreobutr C, Phillion A B, Fife J L and Lee P D 2014 *Acta Materialia* **64** 316
[12] Enz T, Steinbach S, Simicic D, Kasperovich G and Ratke L 2011 *Microgravity Science and Technology* **23** 345
[13] Ferdian D and Lacaze J 2012 *Transactions of the Indian Institute of Metals* **65** 821
[14] Zimmermann G, Schaberger-Zimmermann E, Steinbach S and Ratke L 2014 *Materials Science Forum* **790** 40
[15] Noeppel A, Ciobanas A, Wang X D, Zaidat K, Mangelinck N, Moreau R, Weiss A, Zimmerman G and Fautrelle Y 2010 *Metallurgical and Materials Transactions* **B41** 193
[16] Budenkova O et al. 2014 *Materials Science Forum* **790** 46